

The morphology and orientation of polyethylene in films of sub-micron thickness crystallized in contact with calcite and rubber substrates

Z. Bartczak^{1a}, A.S. Argon^{a,*}, R.E. Cohen^a, T. Kowalewski^b

^aMassachusetts Institute of Technology, Cambridge, MA 02139, USA

^bDepartment of Chemistry, Washington University, St. Louis, MO 63130, USA

Received 1 May 1998; accepted 2 June 1998

Abstract

Studies of non-isothermal crystallization morphologies were carried out in thin films of HDPE ranging in thickness of 15 nm–1.2 μm , adjacent to either (104) surfaces of calcite crystals or between thin layers of ethylene–octene rubber, both in support of the two preceding investigations of the toughening mechanism of HDPE with rubber and CaCO_3 particles. Combined WAXS measurements and AFM imaging of the crystallization forms established that, for films of thickness less than 0.3 μm , lamellar crystallites preferentially grew ‘edge-on’, in sheaf-like morphology, on the calcite or rubber interfaces with the (100) crystallographic planes of the lamellae lying parallel to the interfaces. In films thicker than 0.4 μm the characteristic banded spherulitic morphologies of twisted lamellae became dominant. These observations furnish strong support for the toughening mechanism discussed in the two companion studies (I) and (II). © 1999 Elsevier Science Ltd. All rights reserved.

Keywords: Crystallization in thin films; HDPE; Sheaf-like crystallites

1. Introduction

In the two preceding companion communications to be referred to here as I [1] and II [2] we presented results of a detailed study of the mechanism of toughening high-density polyethylene (HDPE) with incorporated heterogeneity particles of: first a series of rubbers (I) and then equiaxed CaCO_3 particles (II). In these studies we demonstrated that a dramatic toughness jump occurs when the thickness of the interparticle matrix ligament becomes smaller than 0.6 μm which is characteristic of HDPE, and was found to be independent of either the type of rubber particle or the nature of the CaCO_3 particle. These findings were very similar to what Muratoglu et al. [3,4] had reported recently for the mechanism of toughening Nylon 6 and 6.6, and strongly reinforced the proposition of Wu [5], that toughness jumps in notch-brittle semi-crystalline polymers are achieved not when certain volume fractions of rubbery components are incorporated, nor when their size falls into a certain range, but when the inter-particle matrix ligament becomes less than a critical dimension. Through detailed and meticulous studies utilizing TEM, WAXS, and tensile

stretching experiments of sub-micron thickness pedigreed films of Nylon 6, Muratoglu et al. [3,4] had demonstrated that when matrix ligaments have thicknesses less than the critical value they possess a highly regular morphology of crystallites with preferred orientation in which the lowest free energy crystallographic planes, having also the lowest slip resistance, lie parallel to the interfaces of the particles. This morphology has a significantly lowered anisotropic plastic resistance. When it percolates throughout the modified blend it results in lowered overall plastic resistance and initiates tough response. In our two companion studies we have demonstrated that the same phenomenology is present also in HDPE. The purpose of the present study is to demonstrate that such preferential crystallization also takes place in PE in interparticle ligaments having a thickness less than 0.6 μm , regardless of whether the interfaces it shares are with rubber domains or CaCO_3 crystals.

The subject of thin polymer films and their properties, however, is far broader than the application to toughening notch-brittle semi-crystalline material. Thus, e.g. in resist layers used widely in the fabrication of micro-electronic devices or in layers of liquid crystal displays, to name just a few, similar considerations arise regarding the properties of polymer films with thicknesses in the range of 0.1–1.0 μm . In addition, the behaviour of a semi-crystalline

* Corresponding author.

¹ Permanent address: Centre of Molecular and Macromolecular Studies, Polish Academy of Sciences, 90-363 Lodz, Poland.

polymer in the form of sub-micron thick layers can also influence the properties of bulk polymers. For example, in semi-crystalline block copolymers exhibiting micro-phase separation, material undergoing crystallization in block form frequently tends to orient with its chain direction parallel to an interface [6–8]. Such specific orientation could influence the barrier properties of the copolymer or some of its mechanical properties. In such thin films the morphology is produced by crystallization from the melt in confined spaces where it is constrained by two interfaces of a second polymer or an inorganic substance [4,9].

Model calculations and computer simulations of the behaviour of polymer chains in confined spaces, as found in thin and ultra-thin films, has demonstrated that conformation of chains, segmental mobility and other properties are greatly influenced by the presence of the interfaces [10–13]. The self-consistent field lattice model calculations of a polypropylene melt on graphite suggested enrichment of the interface with chain ends, some flattening of the chains parallel to the plane of the interface and anisotropic molecular mobilities [13].

Several experimental studies of thin and ultra-thin polymer films have demonstrated that the organization of chains in such films is different than in bulk material. Thus, Prest and Luca [14] found that the birefringence of static-cast films of several amorphous polymers, including polystyrene and polycarbonate (1–5 μm thick, cast on a glass substrate), increased as the film thickness decreased, indicating higher in-plane orientation of the chains in the thinner films. Cohen and Reich [15] also reported some higher planar orientation of chains in the layer near the interface in films of polystyrene dip-coated on a glass substrate. They also found that the long-range order could extend to thicknesses of 10 μm in films of high-molecular weight polystyrene. The investigations of ultra-thin films of amorphous poly(3-methyl-4-hydroxy styrene) formed by spin-coating [16] showed a higher level of bound residual solvent in films thinner than 0.1 μm , which resulted from in-plane orientation of chains producing enhanced intermolecular hydrogen bonding in that layer.

Preferred chain orientation parallel to the substrate plane was found also in crystallites formed in thin films of semi-crystalline polymers such as Nylon-6 [4], Nylon 6.6 [17], poly(di-*n*-hexyl silane) (PD6S) [16,18,9] poly(alkylthiophenes) [19] and poly(aryl ether ketone ketone) (PEKK) [20]. Despotopoulou and co-workers [16,18,21] found a critical thickness of PD6S film of 15 nm, below which the crystallization of the polymer film was completely inhibited. For thicker films the crystallization kinetics and resulting degree of crystallinity were strongly influenced by the film thickness. In the range of film thickness of 0.15–2.0 μm the rate of crystallization decreased substantially with decreasing film thickness. The change of the overall dimensionality of crystallization from three- to one-dimensional growth was also found to occur with decreasing film thickness [19]. Muratoglu et al. [4] probed the crystalline texture of thin layers of Nylon-6 confined between two layers of a

rubber and crystallized from the molten state. They found a well-developed orientation of crystallites with chain axes parallel to the film plane in thin films below 0.3 μm . With increasing film thickness the texture became progressively more diffuse, although a relatively weak preferred orientation was still observed in films of 4.6 μm thickness. This preferred orientation of crystalline component was associated with the layers next to the interface. Moreover, by tensile stretching experiments these authors demonstrated a high level of plastic anisotropy of these thin films exhibiting preferred orientation.

Pan et al. [22] studied multi-layer films composed of alternating layers of PE and PS, obtained by a special extrusion process. The thickness of the PE layers was approximately 20 μm . They found (100) crystallographic planes of PE parallel to the film plane and the molecules aligned in the extrusion direction.

The observations that the in-plane orientation of chains gradually decreases with increasing film thickness (as in amorphous polystyrene and polycarbonate [14,15] or in semi-crystalline Nylon 6 [4]) suggest that similar interface-induced chain organization can be expected in the region adjacent to a polymer/substrate interface in films of any thickness or even in bulk materials in which the interfaces are present (e.g. block copolymers or polymer blends and composites). This would lead to substantial, or in some cases even dramatic modification of the properties of these materials [9]. Therefore, systematic probing of the chain organization in thin and ultra-thin films, particularly near interfaces, should lead to important understanding of key phenomena because of the potential influence on a variety of properties of heterogeneous materials in bulk.

Thus, the aim of the present study was not only to furnish key morphological detail in support of our associated toughening studies (I and II) [1,2] but also probe, to some extent, the crystallization habits of semi-crystalline polymers and the resulting molecular orientation in near-interface layers of thin films deposited on either amorphous or crystalline substrates. The polymer chosen for this study was linear polyethylene, first because this was the material of concern in (I) and (II) but also because it is a very attractive model material with a relatively simple structure, and free from heteroatoms or hydrogen bonds, which could produce unusual, specific interactions. The substrates of amorphous rubber and crystalline calcite (calcium carbonate) were chosen not only to furnish direct support for our studies in (I) and (II), but also because they represent the two most widely used groups of polymeric modifiers and mineral fillers, respectively.

2. Experimental details

2.1. Materials and preparation of thin films

The polyethylene used in this study was high-density polyethylene (HDPE) Dowlex IP-10, supplied by Dow

Chemicals. It has a density of 0.962 g/cm^3 (annealed) and melt flow index of 9 g/10 min (2.16 kG at 190°C). Thin films of thickness ranging from 15 nm to $1.2 \mu\text{m}$ were prepared by spin-coating from hot xylene solution ($100\text{--}110^\circ\text{C}$) on $2 \times 2 \text{ cm}$ substrates preheated to 120°C . Various desired film thicknesses were obtained by varying both the concentration of polymer solution (in the range from 0.5 to 4 wt\%) and the rotation speed of the substrate during the spin-coating process ($1500\text{--}4000 \text{ rpm}$).

Two different substrate types were used for spin-coating. One was a wafer of calcite single crystal cut parallel to the (104) crystallographic plane (supplied by Keon Optics, Stony Point, NY). In several experiments a wafer of silicon single crystal cut parallel to its (100) plane (supplied by Semiconductor Processing Company, Boston, MA) was also used to obtain some comparison. The second substrate type was amorphous rubber (ethylene–octene copolymer, Engage 8200, supplied by DuPont Dow Elastomers) prepared by spin-coating of the rubber film on a silicon wafer. The thickness of the rubber layer was $50\text{--}100 \text{ nm}$. In order to make the rubber layer insoluble it was radiation crosslinked using a dose of 20 Mrad (electrons) prior to casting on it the polyethylene film. After deposition of the polyethylene film of a desired thickness on such rubber substrates a second rubber layer of a thickness of approximately 50 nm was spin-coated on the top of the polyethylene film to produce a sandwich configuration. Fig. 1 shows schematically the layer structure of the prepared samples. Thickness of the polyethylene layer was determined with a profilometer (Dektak 3).

After the preparation of thin films, samples were subjected to a thermal treatment by placing them into a brass chamber that was first evacuated and then filled with argon

gas which was maintained as an inert blanket during the subsequent thermal treatment in order to avoid oxidative degradation of the films. The thermal treatment consisted of placing the brass chamber in an oil bath where it was kept at a temperature of 180°C for 15 min to melt the film. The brass chamber was then taken out of the oil bath and allowed to cool slowly to room temperature. This relatively slow cooling process resulted in non-isothermal crystallization of the polyethylene films. The films deposited on calcite and silicon were not subjected to any further treatment, while in the samples sandwiched between rubber the top layer of rubber was dissolved by washing the top of the sandwich with xylene at room temperature, while the sample was being spun at 3000 rpm . This procedure was quite effective in removing the top rubber layer and left the polyethylene film intact and attached to the lower rubber substrate.

2.2. Atomic force microscopy

A NanoScope III AFM instrument (Digital Instruments, Santa Barbara, CA) equipped with a J-scanner was employed in this study. The J-scanner allowed scans over square areas up to $130 \mu\text{m}$ edge length to be acquired. In most observations, a contact mode was used with AFM NanoProbe tips made of Si_3N_4 (Digital Instruments) on cantilevers with a nominal spring constant of $k = 0.12 \text{ N/m}$. Several scans were made also in a tapping mode.

In the contact mode of operation, height and deflection images were collected. A height image obtained from the scanner position, gives direct information on the topography of the sample surface visualized by the gray scale where white represents the highest points of the sample surface and black the lowest. The deflection image is acquired from the deflection of the cantilever with a probe. The cantilever deflection reflects directly the local slope of the sample topography along the direction of scanning. Hence, the deflection images frequently resemble TEM images of surface replicas, shadowed with metal and may be interpreted similarly. However, to avoid misinterpretation deflection images were always interpreted together with their respective height image.

2.3. X-ray diffraction

The crystallographic orientation of PE in the thin films was probed and measured quantitatively with wide-angle X-ray diffraction (WAXS) by partial pole figure measurements. The measurements were performed on a Rigaku goniometer equipped with pole figure attachment, coupled to a Rigaku RU200 rotating anode X-ray generator with fine point source ($\text{Cu K}\alpha$ radiation). An acceleration voltage of 50 kV and tube current of 60 mA were used.

The partial pole figure technique was used to determine the orientation of polyethylene crystallites in thin film

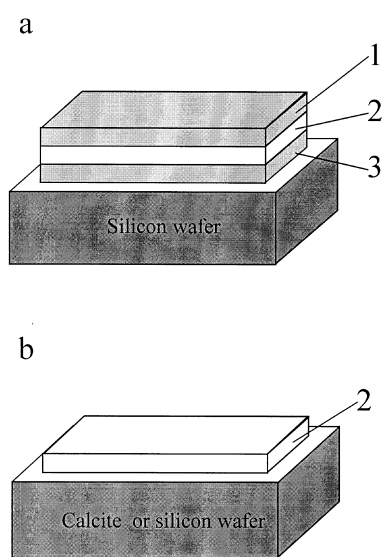


Fig. 1. Schematic drawing of the spin-coated layers of the samples prepared: (a) rubber–HDPE; (b) calcite–HDPE and silicon–HDPE. (1) Cross-linked EOR rubber layer $0.1 \mu\text{m}$ thick; (2) HDPE layer of the thickness of $15 \text{ nm}\text{--}1.2 \mu\text{m}$; (3) EOR rubber layer 50 nm thick; (S) silicon wafer substrate of (100) orientation; (C) calcite wafer of (104) orientation.

samples. The measurements were performed only in the reflection mode in the range of the polar angle, δ from 0 to 75° (where δ represents the angle between the normal to the diffracting plane and that of the surface of the film). The thin films supported on relatively thick substrates could not be probed in transmission. Moreover, detachment of the films from the substrate was both very difficult, and even if successful, such measurements on thin films in transmission would give too low a signal-to-noise ratio to be considered as reliable. Preliminary measurements revealed that the orientation distribution of tested specimens were axisymmetric with respect to the normal to the film plane. Therefore, determination of a pole figure in a full range of azimuthal angles was not necessary and a partial pole figure, measured at a single azimuthal angle, was sufficient for characterization of orientation of crystallites (texture) in the sample. Nevertheless, for every sample investigated a preliminary check of the orientation was made by measurements performed at one polar and a few azimuthal angles to ascertain that the texture of that particular sample had a symmetry axis. The range of polar angle, δ was usually scanned with 5° step increments (10° for a few specimens). For every sample tilt the $\theta/2\theta$ scans were recorded to determine the integral intensities of the (110) and (200) diffraction peaks of orthorhombic polyethylene. These 2θ scans were made ranging from 20° to 25.5° with steps of 0.05°. Appropriate narrow receiving and scattering slits were used for these scans. The collection time for each step was 180–240 s, depending on the film thickness. From the recorded scan, the integral intensities of the diffraction peaks and the integral background were calculated for each polar (tilt) angle by a fitting and peak separation procedure, using a Pearson VII profile for diffraction peaks and linear background approximation. If the scattering from the amorphous phase and/or the monoclinic form of PE were discernible in the scan, their contributions were taken into account in the fitting and a separation procedure was applied in the determination of the (110) and (200) integral intensities. The integral background determined for each tilt angle was used in calculating corrections for instrumental defocusing of X-rays due to the specific sample tilt. The ratio of the integral background measured at $\delta = 0^\circ$ to the background at a given angle δ was taken as the correction factor for defocusing, and the integral diffraction intensities of the (110) and (200) peaks were multiplied by this factor to get the corrected values. Next, these corrected intensities were normalized by dividing them by the average corrected intensity, calculated over the whole range of δ . From the normalized intensities the partial pole figures of (110) and (200) crystallographic planes were constructed and plotted. The average intensity used for normalization may be considered as equivalent to the intensity of diffraction from the randomly oriented specimen. Therefore, the units on the intensity scale in partial pole figures represent multiples of diffraction intensity of the same material with a random orientation of crystallites (m.r.d. units).

3. Experimental results

3.1. Morphology of thin films

The morphology of the films crystallized from the melt was studied by probing the top surface of the films with the atomic force microscope (AFM). The AFM has an advantage over other microscopy techniques, since it does not

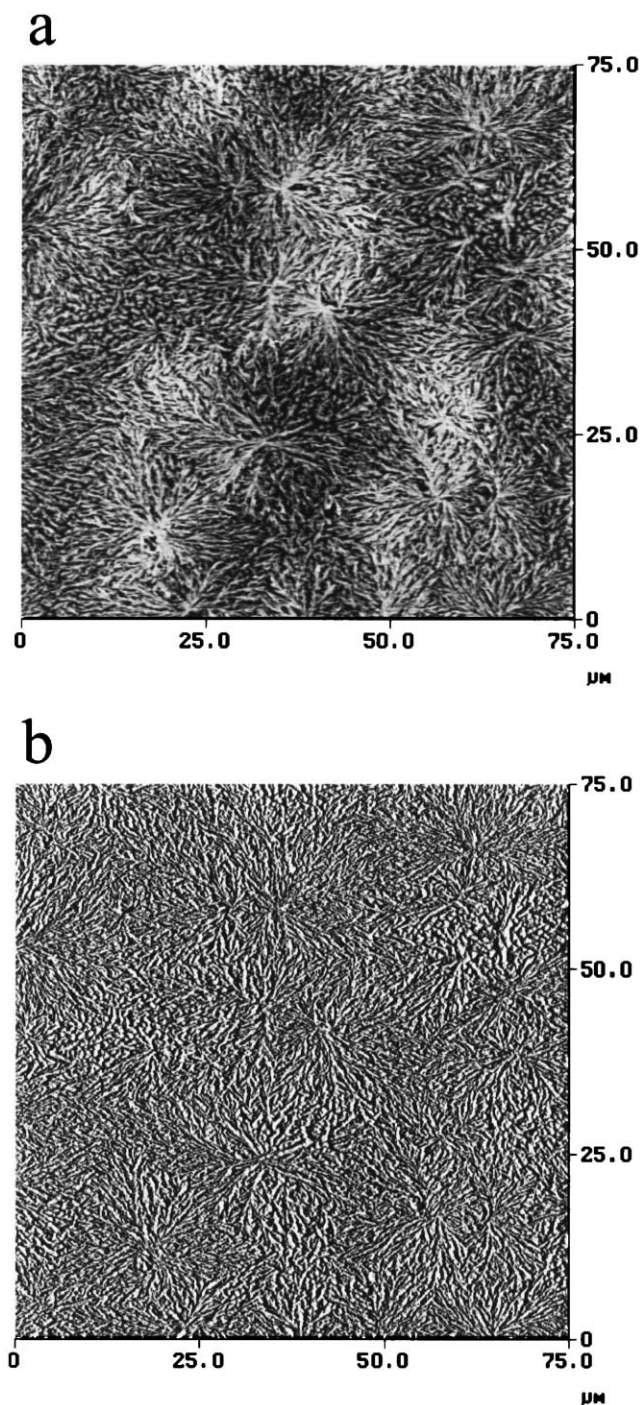


Fig. 2. Contact mode AFM: (a) height image; (b) deflection image of the 15 nm thick polyethylene film spin-coated on calcite substrate. Scan size 75 μm .

require any sample preparation prior to observations, such as etching or staining, treatments which could possibly alter some of the morphological features of the films or produce artifacts.

Fig. 2a and Fig. 2b present AFM height and deflection images, respectively, of the surface of a 15 nm thick film of HDPE cast by spin-coating on a calcite substrate and not subjected to any subsequent thermal treatment. The as-cast polyethylene forms a macroscopically continuous film with uniform thickness. The morphology of the film is composed of sheaf-like aggregates of lamellae of substantially 2D nature. The lamellae within these aggregates form a relatively coarse and open structure and do not fill completely the volume of the film. No dewetting or droplet type aggregation phenomena were observed. The same morphology, although with finer lamellar structure, filling space better within the aggregates was found also in other cast films of larger thickness where the morphology eventually approached closer to those of 3D spherulitic forms. Remelting, followed by re-crystallization of these very thin films, resulted in a variety of dewetting forms and formation of droplets. These will be discussed by some of us elsewhere.

The samples of HDPE cast on (104) calcite crystal surfaces with initial film thickness of 0.1 μm , and above, were found to be continuous, and remained so after some thermal treatment, showing only very occasional local dewetting in the form of holes in the annealed film. Such local dewetting was usually induced by foreign particles. Fig. 3a–d show the morphology of these films after nonisothermal crystallization. It can be observed in the AFM deflection images shown in these figures that the morphology of the melt-crystallized films changes substantially with the change of the film thickness. Two different types of morphology can be distinguished: in films with thicknesses of 0.1, 0.2 and 0.4 μm (Fig. 3a–c, respectively) the lamellae grown in the films continue to be oriented preferentially edge-on and are organized in sheaf-like aggregates oriented randomly in the plane of the films, while in films of larger thickness (0.6 μm , presented in Fig. 3d, and 1.2 μm , not shown here) the morphology more and more approaches that of the well-known spherulitic form with a banded structure, characteristic of linear polyethylene crystallized from the melt at moderately high undercooling, eventually becoming the same as those observed in crystallization of thick films and in bulk samples.

In thin films with the sheaf-like morphology, the aggregates completely fill the film. These sheaf-like aggregates grew from primary nucleation centres similar to primary nuclei found in spherulitic crystallization [23]. They resemble the structures found in the initial stages of spherulitic growth from primary nuclei [18], except that they are much larger and less branched than spherulites in the initial growth stage. The characteristic feature of these aggregates is their nearly unidirectional growth with only little divergence sideways. The lamellae growing from the nucleation

centre are nearly straight and are neither twisted nor branched, maintaining their edge-on orientation from the aggregate centre up to the point of growth termination at the boundary with other aggregates, and across the entire cross-section of the film. The AFM images of film samples thinner than 0.4 μm , presented in Fig. 3a–c, demonstrate this substantial suppression of branching and twisting tendencies compared to the lamellae observed in spherulites in thicker films, such as films of 0.6 μm thickness, presented in Fig. 3d, and above, or in bulk samples. The 2D features must be attributed to the presence of the interface plane between the polymer and the substrate that governs the processes. Thus, it can be inferred that the interface either induces a notable suppression of the mechanism responsible for branching or, which seems more probable, induces an increase of the growth rate (i.e. rate of the secondary nucleation) of the lamellar crystallites oriented specifically edge-on against the interface plane. Apparently, the growth of lamellae of other orientations, not having the benefit of the interface, is overwhelmed by the more rapidly growing ones that are influenced by the interface. As a result, the branching and twisting become largely suppressed due to kinetic reasons. The very limited branching causes the transformation of the morphology of aggregates into the sheaf-like 2D forms.

In contrast, in films of larger thickness, such as that of 0.6 μm thickness, shown in Fig. 3d, and in a film of 1.2 μm thickness, the observed morphology more closely resembled that of a spherulite. The lamellae within spherulites are extensively branched, and regularly twisted, which produces complete filling of the space and a characteristic banded pattern. The twisting adversely affects the preferential form of crystallization, dominant in thin films. The change of the morphology with increasing film thickness demonstrates that the influence of the substrate on the crystallization process is limited to a layer of a few tenths of a micron, estimated as about 0.2–0.4 μm from the interface. At larger distances from the interface the inevitable branching of lamellae causes transformation of the morphology of the film to spherulitic. However, in a thin layer near the interface even in thicker films the crystallization proceeds similar to that observed in the thinner films, reported above.

Practically identical morphologies to those reported above were observed in thin films of polyethylene crystallized on silicon substrates. The transition from the spherulitic to sheaf-like morphology was observed at the same thickness range, i.e. near 0.4 μm . Similar to the films crystallized on calcite, the sheaf-like aggregates were oriented randomly in the plane of the film, while lamellae within these aggregates were oriented preferentially edge-on.

Morphological features similar to those observed in PE films crystallized on crystallographic substrates of calcite and described above, including the transformation of the morphology from spherulitic to the sheaf-like forms with decreasing film thickness, were observed also in films of HDPE crystallized between two thin rubber layers. The

AFM images of these films (with the upper rubber layer removed (dissolved) prior to examination) are presented in Figs 4 and 5. Fig. 4 shows AFM images of a $0.2\ \mu\text{m}$ film of PE crystallized between two EOR rubber layers, where the lamellae are seen to grow edge-on against the rubber substrate, with only little branching and twisting, which leads to the formation of sheaf-like aggregates. Fig. 5a,b shows a film of $0.6\ \mu\text{m}$ thickness crystallized between two rubber layers. It now shows the

characteristic banded spherulitic morphology of periodically twisted lamellae.

3.2. Orientation of crystalline component

Fig. 6a presents a pole figure of the (110) crystallographic plane of orthorhombic polyethylene obtained for a $0.1\ \mu\text{m}$ thick film of HDPE cast on (104) calcite wafer surfaces, after re-melting and subsequent recrystallization

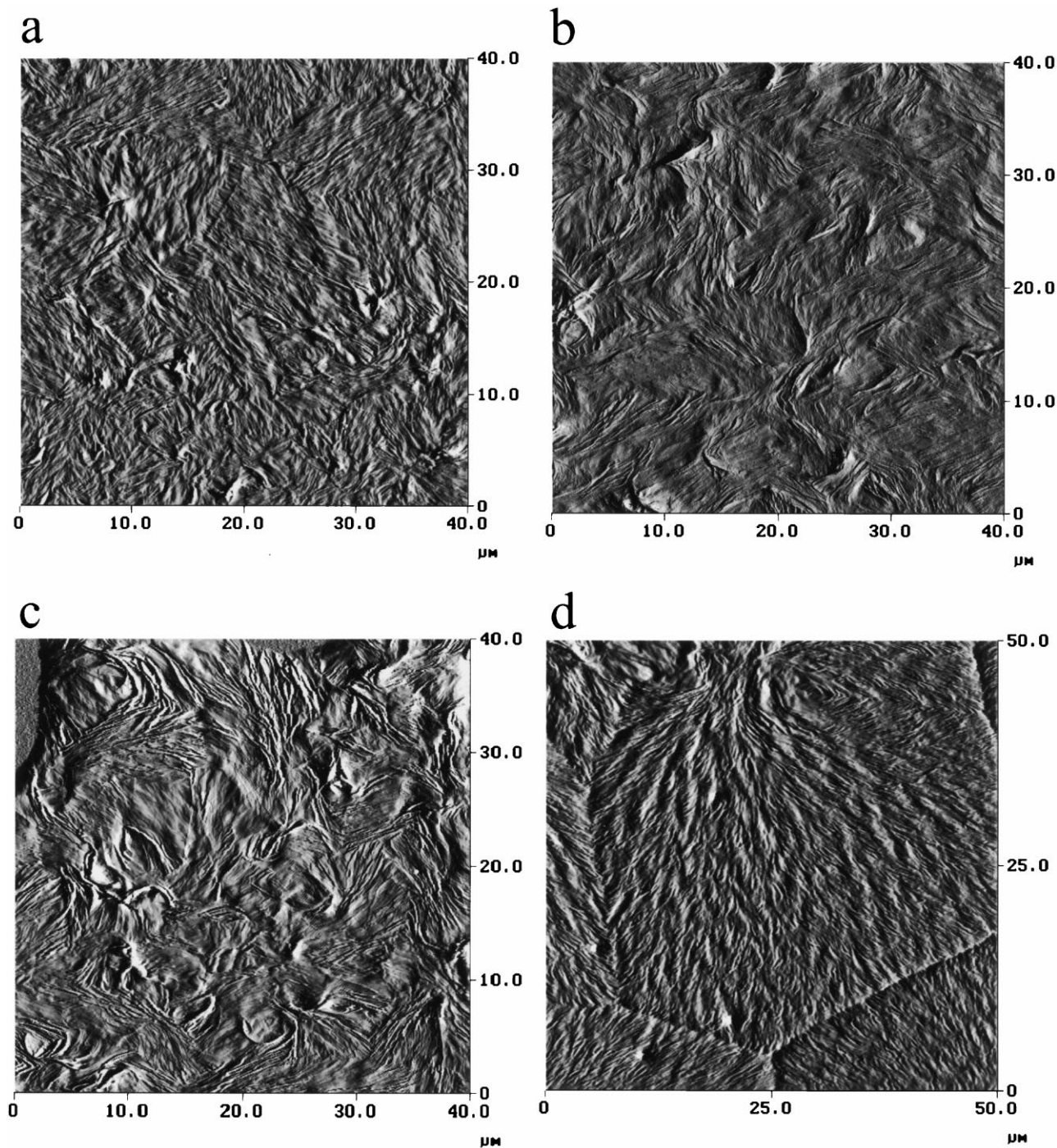


Fig. 3. Contact mode AFM deflection images of thin films of HDPE crystallized on calcite surface with the film thicknesses of: (a) $0.1\ \mu\text{m}$, (b) $0.2\ \mu\text{m}$, (c) $0.4\ \mu\text{m}$ and (d) $0.6\ \mu\text{m}$. Scan size $40\ \mu\text{m}$.

at non-isothermal conditions. Fig. 6b shows a set of partial pole figures of this diffracting plane constructed from the same experimental data for several azimuthal angles. Both full and partial pole figures demonstrate that the texture of the polyethylene in this thin film sample has a symmetry axis coincident with the substrate plane normal. The measurements of other samples demonstrated that such an axial symmetry of the orientation of (110) and (100) planes was present in all samples investigated. Therefore, the partial pole figures determined for any azimuthal angle completely characterize the texture of the crystalline component.

Fig. 7a–e shows the (110) and (200) normalized partial pole figures of HDPE films crystallized from the melt on a

calcite substrate. The films had thicknesses of 0.1, 0.2, 0.4, 0.6 and 1.2 μm , respectively, with morphologies of the four thicknesses shown in Fig. 3a–d. The dashed line on each plot at unit intensity represents a randomly oriented sample. These figures demonstrate that all films in the thickness range investigated have some non-random texture, and this texture is the strongest in the thinnest film of 0.1 μm thickness. Maxima of diffraction intensity at the direction of preferred orientation of both (110) and (200) planes are sharp and about five times higher than the intensity of a random specimen (see Fig. 7a where normalized intensity is expressed in random diffraction (m.r.d.) units). The sharp maximum of the orientation of (200) planes is located at the

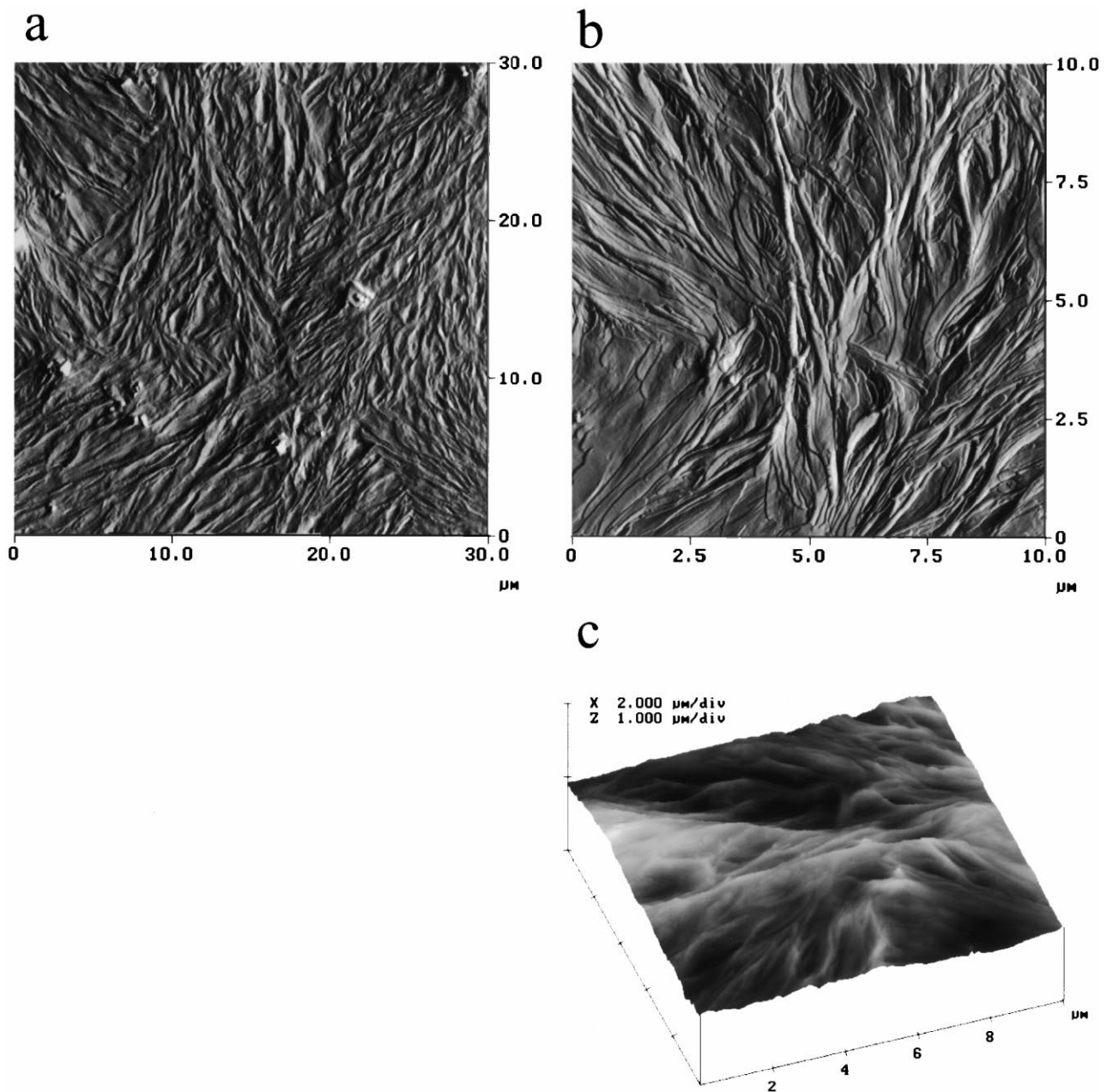


Fig. 4. Contact mode AFM image of HDPE film of 0.2 μm thickness, crystallized between two layers of EOR rubber; (a) deflection image, scan size 30 μm ; (b) deflection image; and (c) height image of another region of the same specimen, scan size 10 μm .

polar angle, $\delta = 0^\circ$, which suggests that the orientation of the (200) plane, containing the chain axis, is parallel to the film surface (i.e. a texture of (100) type). Additionally, this maximum has a relatively broad plateau on its shoulder extending up to the polar angle of 40° , which suggests the presence of an additional texture component, but much weaker than the main component at $\delta = 0^\circ$. The axial symmetry around the normal to the film plane (cf. Fig. 6)

indicates that there is no preferred direction of orientation of chains within the plane of the film. The partial pole figure of (110) plane shows a well-developed maximum near $\delta = 65^\circ$. The angle between normals to (100) and (110) planes calculated on the basis of the size of the unit cell of orthorhombic polyethylene [24] is approximately 56° , so that for an ideal, one-component texture of (100) type, one could expect a maximum observable experimentally at a considerably higher value of δ . This must be because the texture observed is not an ideal one of (100) type, and there is a considerable misalignment and tilting of a fraction of crystallites from their ideal orientation having the (100) plane parallel to the film plane, suggested by the broad plateau in (200) pole figure mentioned earlier. The misalignment in the crystallites results in the formation of a shoulder on the maximum of the (200) orientation and a shift of the (110) maximum toward higher angles.

The texture observed for the $0.2 \mu\text{m}$ thick film (see Fig. 7b) is of the same type as in that of the $0.1 \mu\text{m}$ thick film, although it is more diffuse—the maxima of orientation of the (200) and (110) planes are broader than in the film of $0.1 \mu\text{m}$ thickness, while their height decreases to less than 4 m.r.d; all indicative of a morphological dilution of orientational perfection. For thicker films (0.4 , 0.6 and $1.2 \mu\text{m}$, Fig. 7d,e) the orientation of crystallites becomes progressively more diffuse and, eventually, only a trace of the preferred orientation can be detected in the film of $1.2 \mu\text{m}$ thickness, with the intensity at maxima being only around 1.5 m.r.d. This relatively low orientation results probably from a stronger orientation present only very near the interface as in the thinner films, and much weaker or completely random orientation away from that interface that causes the morphological dilution referred to above.

The orientation features, similar to those described above, can also be found in HDPE films crystallized between two amorphous rubber layers. The respective partial pole figures are presented in Fig. 8a–d for thicknesses of HDPE films of 0.1 , 0.2 , 0.6 and $1.2 \mu\text{m}$, respectively. The principal textures, especially those detected in the thinnest films of 0.1 and $0.2 \mu\text{m}$ thickness, are again of the type of (100) with the symmetry axis around the normal to the film plane, i.e. (100) planes are oriented preferentially parallel to the plane of the film with no preferred orientation direction existing for the chain within this plane. For the $0.6 \mu\text{m}$ thick film that texture is considerably weaker, while for the film of $1.2 \mu\text{m}$ the preferred orientation nearly disappears entirely and the orientation of the (200) and (110) planes is very close to being random. Although the texture detected in the HDPE films crystallized against substrates of an amorphous rubber is essentially of the same type as found in HDPE crystallized against calcite crystals (and silicon) substrates, the comparison of the heights of maxima and widths of respective pole figures demonstrates that this orientation is weaker and more diffuse than in the case of crystallization against calcite substrates.

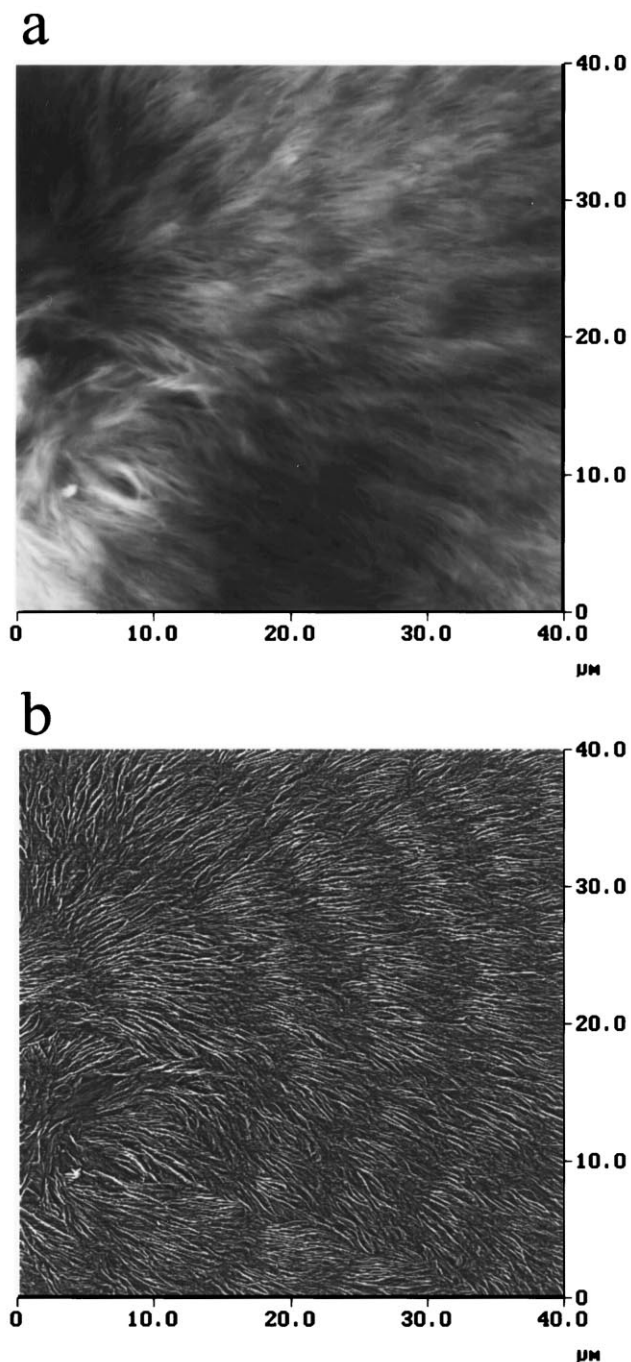


Fig. 5. Contact mode AFM image of HDPE film of $0.6 \mu\text{m}$ thickness, crystallized between two layers of EOR rubber: (a) height image; (b) the same image after filtering with highpass filter to visualize banded appearance of the spherulite. Scan size $40 \mu\text{m}$.

Such a difference is explainable, since the interface between polyethylene and rubber at the time of crystallization is an interface between two liquids, and its influence on the crystallization process could be weaker than the influence of an interface between a molten polymer and a crystalline solid. Nevertheless, the transition from relatively sharp to diffuse texture can be observed at a film thickness below $0.6 \mu\text{m}$, i.e. in the same range of thickness as observed in the films crystallized against calcite substrates.

4. Discussion

4.1. Morphology of thin films

The morphological studies demonstrated that for every film thickness and substrate type the crystallization of the film was initiated by formation of primary nuclei followed by a growth stage. The primary nuclei formed preferentially on the bottom surface of the film contacting the crystalline or the rubber substrate since better heat transfer from the bottom film surface through the substrate existed in the brass crystallization cell than from the top surface in contact with the gas blanket. The AFM observations revealed that, in the case of the polyethylene film sandwiched between rubber layers, the upper layer was practically inactive as a source of primary nuclei. Therefore, the effect on crystallization of the calcite surface and the PE/rubber interface can be considered to be essentially identical, with the only difference in the type of the substrate.

For both cases of crystalline or amorphous substrate the morphology of the crystalline component of polyethylene film changes in a similar fashion with increasing film thickness. In films of thickness up to $0.4 \mu\text{m}$, crystallization leads to the formation of sheaf-like aggregates in which lamellae

are very little branched and/or twisted and are oriented predominantly edge-on with respect to the substrate surface. Such orientation is maintained across the entire cross-section of the film. In the films of $0.6 \mu\text{m}$ thickness and larger, the morphology reverts to conventional spherulites, resembling progressively those found in bulk crystallization. The X-ray diffraction pole-figure studies demonstrate that the change from sheaf-like to spherulitic morphology is accompanied by the transformation of the preferred crystallographic orientation from a relatively sharp (100) planar texture to a much more diffuse orientation pattern—albeit still resembling the same (100) texture type. The weaker orientation of crystallites in the thicker spherulitic films is due to extensive branching of the lamellae and twisting along their length.

In thin films exhibiting a sheaf-like morphology the lamellae were found to be oriented preferentially edge-on against the substrate, i.e. with their normals either parallel to the plane of the substrate or, found more frequently, somewhat tilted with respect to the plane. The X-ray orientation studies revealed a strong preferred orientation of the (100) crystallographic plane, containing chain axes, as parallel to the substrate plane. In the 0.1 and $0.2 \mu\text{m}$ thick films this texture is relatively sharp. Both lamella and chain axis orientations found are consistent since the chain axis and lamella normals in polyethylene lamella crystals are known to often form an acute angle in the range of 20 – 40° depending on the condition of crystallization [25].

The reason for such specific lamellar morphology in thin films is most probably the influence of the substrate on the secondary nucleation process controlling the crystal growth. When the lamellar crystal grows in bulk, away from the substrate, the formation of a secondary nucleus on the growth face of the crystal does not depend on the location of the nucleus on that face. The change of free enthalpy on the formation of a secondary nucleus then can be expressed

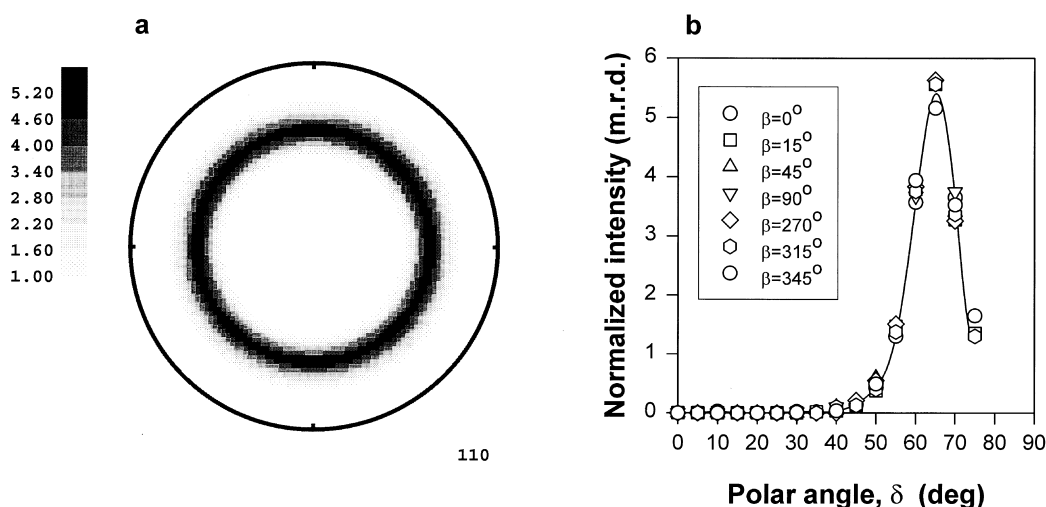


Fig. 6. (a) Full pole figure; and (b) respective partial pole figures of (110) plane of polyethylene, measured for $0.1 \mu\text{m}$ thick HDPE film crystallized on calcite (104) wafer. The points in (b) represent partial pole figures measured for the azimuthal angles of 0 , 15 , 45 , 90 , 270 , 315 and 345° .

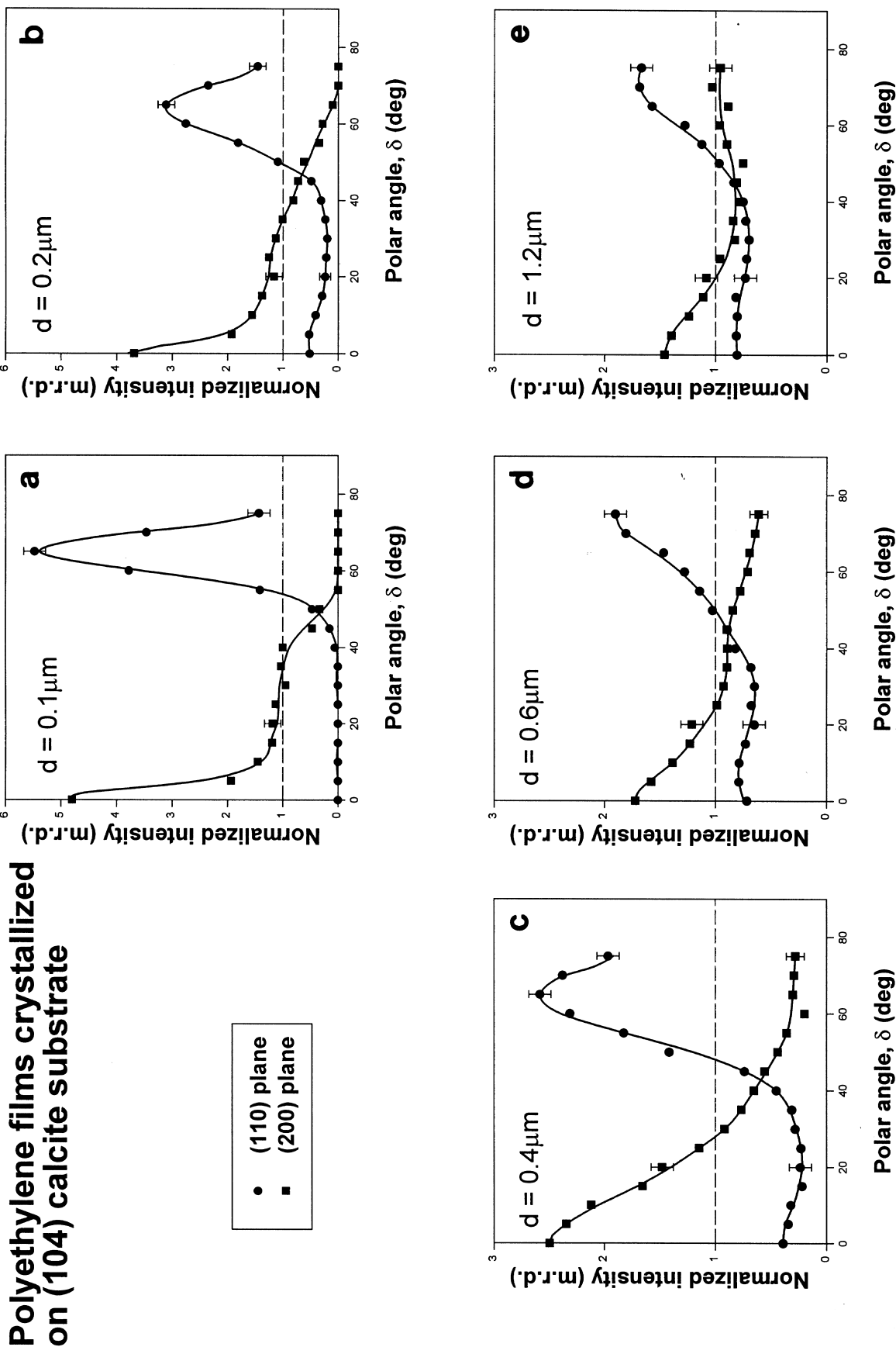


Fig. 7. The partial pole figures of (110) and (200) planes (circles and squares, respectively) determined for thin films of HDPE crystallized on calcite substrate. The film thicknesses were: (a) 0.1, (b) 0.2, (c) 0.4, (d) 0.6 and (e) 1.2 μm .

according to the classical nucleation concepts [23]:

$$\Delta G = -ab_0l\Delta g_f + 2b_0l\chi_{cm} + 2ab_0\chi_e \quad (1)$$

where a , b_0 and l are the width, thickness (equal to that of a monolayer) and length of the nucleus, respectively, Δg_f is

the free enthalpy of melting, χ_{cm} is the interfacial free energy between a lateral crystal plane and the polymer melt, and χ_e is the interfacial free energy between the folding plane of the crystal and the polymer melt. From Eq. (1) the energy barrier for critical nucleus formation can then be

Polyethylene films crystallized between 2 rubber layers (EOR)

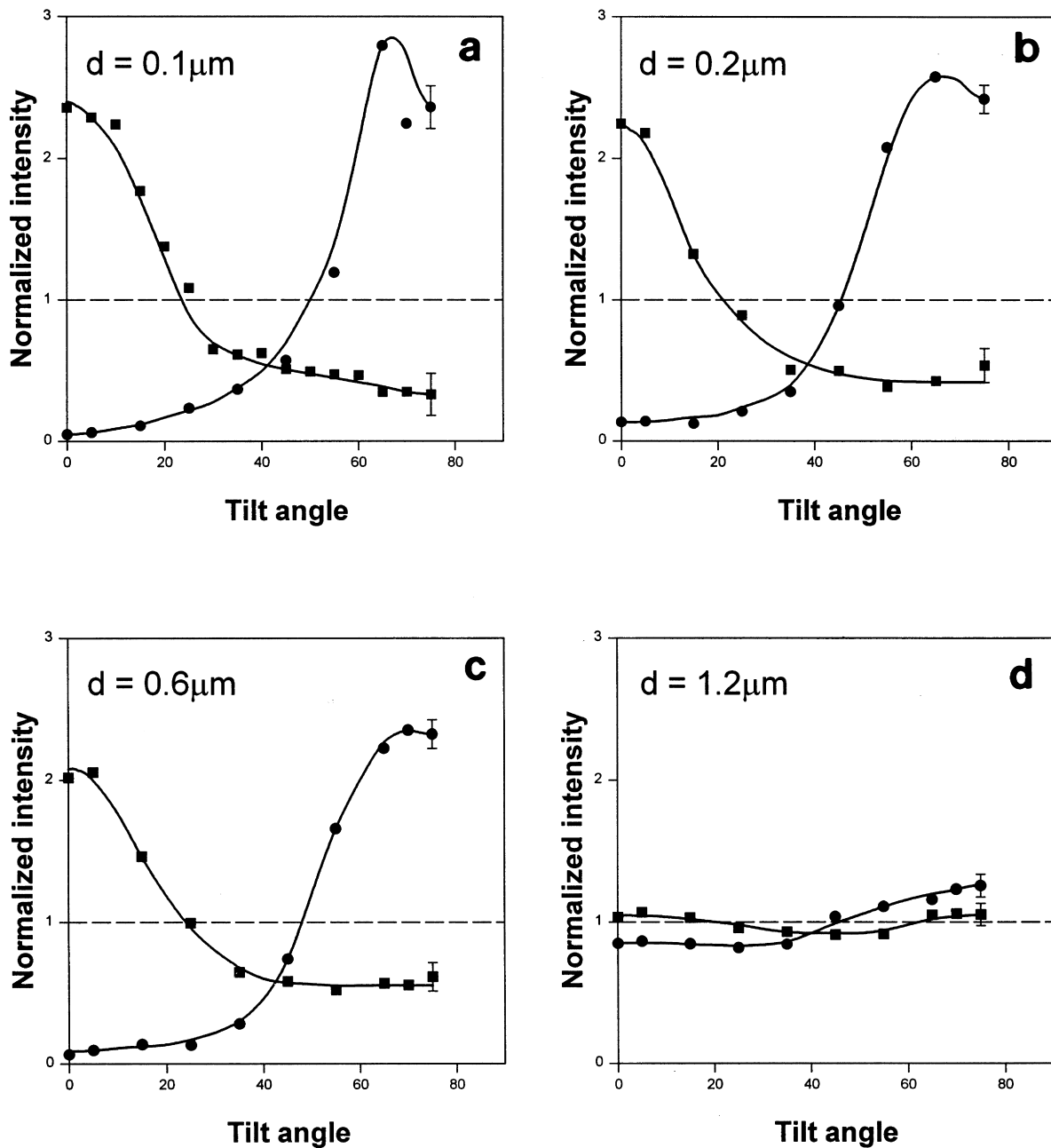
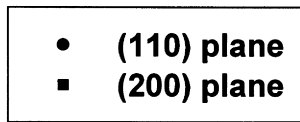


Fig. 8. The partial pole figures of (110) and (200) planes (circles and squares, respectively) determined for thin films of HDPE crystallized between two rubber substrates. The film thicknesses were: (a) 0.1, (b) 0.2, (c) 0.4 and (d) 1.2 μm.

obtained as:

$$\Delta G^* = 4b_o\chi_{cm}\chi_e/\Delta g_f \quad (2)$$

The rate of secondary nucleation and hence the linear growth rate of the lamella are then governed by a characteristic rate expression $\exp(-\Delta G^*/kT)$ [23].

In contrast, when the lamellar crystal grows in contact with the substrate, as in the present study, the change of free enthalpy of formation of a secondary nucleus depends on the location of that nucleus on the plane of growth. If the nucleus is not in contact with the substrate (as the nucleus marked (a) in Fig. 9) the free enthalpy change is the same as that for the crystal growing away from the substrate, consequently, ΔG and ΔG^* are described by Eq. (1) and Eq. (2), respectively. However, if the nucleus forms in the re-entrant corner formed by the substrate and the growing crystal face (position (b) in Fig. 9) Eq. (1) and Eq. (2) have the form:

$$\Delta G = -ab_o l \Delta g_f + b_o l (\chi_{cm} + \chi_{cs} - \chi_{ms}) + 2ab_o \chi_e \quad (1a)$$

$$\Delta G^* = 2b_o (\chi_{cm} + \chi_{cs} - \chi_{ms}) \chi_e / \Delta g_f \quad (2a)$$

where χ_{cs} and χ_{ms} are the interfacial free energy between the lateral plane of the crystal and the substrate, and between the polymer melt and the substrate, respectively. From Eq. (1) and Eq. (1a) the dimensions of the critical nucleus can be estimated. The length (along the chain direction) is the same for both (a) and (b) types of nuclei (cf. Fig. 9):

$$l^* = 2\chi_e / \Delta g_f \quad (3)$$

while the width for nucleus (a) (bulk crystallization) is:

$$a^* = 2\chi_{cm} / \Delta g_f \quad (4)$$

and for nucleus (b):

$$a^* = (\chi_{cm} + \chi_{cs} - \chi_{ms}) / \Delta g_f \quad (4a)$$

Comparison of Eq. (2a) and Eq. (2) indicates that the energy barrier for formation of a critical sized nucleus in a re-entrant corner between the crystal plane and the substrate (Eq. (2a)) may be lower than the respective barrier for formation of such a nucleus away from the substrate or in bulk crystallization (Eq. (2)), provided that

$$\chi_{cs} - \chi_{ms} < \chi_{cm} \quad (5)$$

The same conclusion follows from a comparison of Eq. (4a)

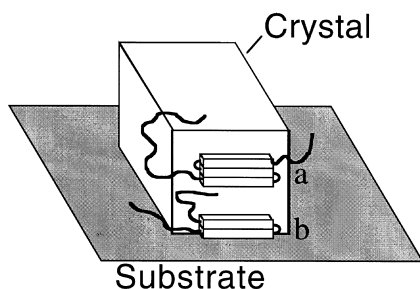


Fig. 9. Two possible secondary nucleus types: (a) formed on the face of growing lamellar crystal, away from the substrate; and (b) formed in the re-entrant corner between lamella face and substrate.

and Eq. (4), that the critical dimension of the nucleus formed in contact with the substrate is smaller than that in bulk when condition (5) is satisfied.

Condition (5) can be satisfied for many different substrates. The considerations of primary heterogeneous nucleation yields analogous conditions [26], and various (stronger or weaker) nucleation activity was demonstrated for numerous other substrates [26,24]. We should note here that the substrates used in the present study, i.e. calcite and ethylene–octene rubber exhibit some, albeit very weak, heterogeneous nucleation activity towards linear polyethylene which manifests itself in a slight increase of temperature of a non-isothermal crystallization peak observed by d.s.c. in the blends of HDPE with calcium carbonate (calcite) particles and rubber [1,2].

In films of thickness comparable with the lateral dimensions of lamellae, the most effective and fast conversion of melt into crystalline component is when the lamellae grow along the substrate, since the same degree of conversion can be accomplished with smaller number of primary nuclei than in the case of growth of lamellae outwards from the substrate.

In the case, when condition (5) is satisfied for a given polymer/substrate pair, the rate of secondary nucleation, of the crystals growing in contact with the substrate and oriented edge-on is larger than of those growing without such contact or lying flat on the substrate. The result would be a faster growth of edge-on lamellae along the substrate plane than lamellae of any other orientation, or those growing in bulk. Twisting of the lamellae growing in this fashion should be substantially reduced in comparison with lamellae growing in bulk, since twisted lamellae lose contact with the substrate and consequently slow down their growth to the bulk growth rate. Thus, the lamellae growing on the interface will consume all the melt accessible to the growing front of adjacent twisted lamellae, due to the limited supply of melt in the film with thickness comparable with the lateral size of the lamellae. This causes termination of further growth of twisted lamellae, at the benefit of the 'edge-on' lamellae that continue their fast growth until the local melt is exhausted.

Consequently, the preferred growth habit in thin films crystallized on substrates satisfying condition (5) should be a growth of lamellae in contact with the substrate and maintaining an 'edge-on' orientation with growth parallel to the substrate plane. As a result the morphology of the crystalline aggregates growing in thin films on such substrates should be in the form of sheaf-like aggregates. In thicker films in which degrees of freedom permitting twisting open up, twisted lamellae giving rise to banded spherulites should begin to dominate, while near the substrate edge-on lamellar morphology should remain present. The X-ray studies of orientation are in support of this scenario, showing that in films of 1.2 μm thickness some preferred orientation of crystallites continue to exist in the samples, which must be those adjoining the substrate.

4.2. Consequences of morphology on toughness

Our study of morphology in thin PE films crystallized in contact with substrates of calcite single crystals and rubbers provides the definitive background to our associated studies (I) and (II) on the toughening of HDPE with rubber and CaCO_3 particles. The common denominator of the toughening mechanism, as noted first by Wu [5] is that the toughness jump requires that interparticle matrix ligaments have thicknesses Λ less than a characteristic thickness Λ_c which for PE is found to be approximately $0.6 \mu\text{m}$. In earlier studies of Muratoglu et al. on Nylon 6 and 6.6 [3,4] it was demonstrated that in that material the characteristic ligament thickness was $0.3 \mu\text{m}$, and that the morphology of material of that thickness was in the form of sheaf-like 2D aggregates growing edge-on, on the rubber substrate with the (001) planes of lowest free energy and lowest plastic shear resistance of monoclinic Nylon lying predominantly parallel to the substrate. Based on measurements of the plastic resistance of free-standing sub-micron films of Nylon 6 it was conjectured by these authors that the plastic resistance of ligaments in certain sectors around spherical particles should be substantially lower, and that when such material percolates throughout the blend the overall plastic resistance of the blend would also decrease substantially resulting in tough behaviour. That this is indeed so has been confirmed with special finite element simulations of Tzika et al. [27], using appropriate anisotropic flow criteria. Thus, with our present morphology study, reinforcing the associated toughening studies of (I) and (II) we conclude that the same mechanism of toughening present in Nylon is also present in HDPE, and since the ligament morphology is only dependent on its thickness and not the type of substrate material, the chemistry of the latter is unimportant in achieving the dramatic toughening effects.

We emphasize that the mechanism of toughening based on the ligament thickness threshold in the cases we have considered is governed by the crystalline morphology of this material and that our explanations apply specifically to material of this constitution. As we have discussed in Section 1 there have been many reports that, even in glassy polymers, there is considerable short-range order in material solidified near flat inorganic surfaces. These may or may not be relevant in relation to other reports in the literature that the critical ligament thickness condition on toughening applies more generally. If this is correct, it is necessary that the constitution of such material be carefully studied and that the features of the toughening process be fully reported, such as presence of crazes, cavitation of particles, distortion of cavities, etc., before any rush to judgment is made either in support of the mechanism we have discussed or in refutation of it, to explain those findings.

5. Conclusions

The morphology of the crystalline component of HDPE changes with film thickness when it is crystallized in thin

film form on planar substrates. In polyethylene films of thickness above $0.4 \mu\text{m}$ crystallized from the melt the morphology resembles that of conventional spherulites, while in films of smaller thickness the morphology is in sheaf-like aggregates, regardless of the nature of the planar substrate, i.e. whether calcite or rubber. Within these aggregates the lamellae are oriented edge-on with respect to the substrate and twisting and branching of the lamellae are radically reduced in comparison with conventional spherulitic morphology. Thus, the crystallites in such thin films of $0.1\text{--}0.3 \mu\text{m}$ are mostly oriented with their (100) planes containing the chain axis, parallel to the plane of the substrate. In films thicker than $0.4 \mu\text{m}$ beginning to exhibit spherulitic morphology vestiges of such preferred orientation of crystallites was still found, which suggests that also in these thicker films a preferentially oriented growth layer of lamellae must still occur adjacent to the substrate.

The change in the morphology of thin films and the crystalline orientation produced in them were attributed to accelerated secondary nucleation on these lamella and resulted in oriented 'edge-on' growth, parallel to the substrate surface. Such preferential growth has favourable kinetics that stifles growth resulting in branching and twisting of lamellae.

The specific orientation of the type found in the present study on films of linear polyethylene is expected to be a more general phenomenon that governs structure in thin films of other crystallizing polymers. Moreover, it should be present not only in thin films but also in thin matrix ligaments of heterogeneous polymeric systems, like polymer blends or filled polymers.

Orientation of the crystalline component in such thin films can have a profound influence on the mechanical and other important properties of these films since they give rise to strong anisotropy. Such anisotropy can be quite important in many advanced thin-film technologies widely used in the micro-electronics industry. As we have demonstrated in the two preceding companion papers [1,2] the micro-scale orientation effects produced by the presence of incoherent interfaces in the heterogeneous polymeric systems can radically affect the mechanical behaviour of heterogeneous blends to result in new super-tough materials.

Acknowledgements

This research was supported primarily by the MRSEC Program of the National Science Foundation under award No. DMR 94-00334, and has also made some use of the Shared Facilities of the Center for Materials Science and Engineering at MIT supported by the same program. The AFM studies were carried out at Washington University under partial support from a grant from the Office of Naval Research.

References

- [1] Bartczak Z, Argron AS, Cohen RE, Weinberg M. *Polymer* 1999;40:2331.

- [2] .Bartczak Z, Argon AS, Cohen RE, Weinberg M. *Polymer* 1999;40:2347.
- [3] Muratoglu OK, Argon AS, Cohen RE, Weinberg M. *Polymer* 1995;36:921.
- [4] Muratoglu OK, Argon AS, Cohen RE. *Polymer* 1995;36:2143.
- [5] Wu S. *Polymer* 1985;26:1855; Wu S. *J Appl Polym Sci* 1988;35:549.
- [6] Douzinas KC, Cohen RE. *Macromolecules* 1992;25:5030.
- [7] Cohen RE, Bellare A, Drzewinski MA. *Macromolecules* 1994;27:2321.
- [8] Hamley IW, Fairclough JP, Terrill NJ, Ryan AJ, Lipic PM, Bates FS, Town-Andrews E. *Macromolecules* 1996;29:8835.
- [9] Argon AS, Cohen RE, Muratoglu OK. In: Boyce MC, editor. *Mechanics of plastics and plastic composites*. MD vol 68/AMD vol 215. New York: ASME, 1995:177.
- [10] ten Brinke G, Auserre D, Hadziioannou G. *J Chem Phys* 1988;89:4374.
- [11] Kumar SK, Vacatello M, Yoon DY. *J Chem Phys* 1988;89:5206.
- [12] Bitsanis I, Hadziioannou G. *J Chem Phys* 1990;92:3827.
- [13] Theodoru DN. In: Sanchez IC, editor. *Physics of polymer surfaces and interfaces*, ch 7. Boston, MA: Butterworth-Heinemann, 1992.
- [14] Prest WM Jr., Luca DJ. *J Appl Phys* 1980;51:5170.
- [15] Cohen Y, Reich S. *J Polym Sci Polym Phys Ed* 1981;19:599.
- [16] Frank CW, Rao V, Despotopoulou MM, Pease RFW, Hinsberg WD, Miller RD, Rabolt JF. *Science* 1996;273:912.
- [17] Scott RS. *J Appl Phys* 1957;28:1089.
- [18] Despotopoulou MM, Miller RD, Rabolt JF, Frank CW. *J Polym Sci Polym Phys Ed* 1996;34:2335.
- [19] Fell HJ, Samuelsen EJ, Als-Nielsen J, Grubel G, Mardalen J. *Solid State Commun* 1995;94:843.
- [20] Ho R-M, Honigfort P, Lin H-S, Cheng SZD, Hsiao BS, Gardner KH. *Polymer* 1997;38:5051.
- [21] Despotopoulou MM, Frank CW, Miller RD, Rabolt JF. *Macromolecules* 1996;29:5797.
- [22] Pan SJ, Im J, Hill MJ, Keller A, Hiltner A, Baer E. *J Polym Sci Polym Phys Ed* 1990;28:1105.
- [23] Wunderlich B. *Macromolecular physics*, vol 2. New York: Academic Press, 1976.
- [24] Brandrup J, Immergut EH, editors. *Polymer handbook*, vol 13, 2nd ed. New York: Wiley-Interscience, 1975.
- [25] Voigt-Martin G, Mandelkern L. *J Polym Sci Polym Phys Ed* 1984;22:1901.
- [26] Binsbergen FL. *J Polym Sci Polym Phys Ed* 1973;11:117.
- [27] Tzika P, Boyce MC, Parks DM. (to be published).